Self-focusing and Raman scattering of laser pulses in tenuous plasmas

Cite as: Physics of Fluids B: Plasma Physics **5**, 1440 (1993); https://doi.org/10.1063/1.860884
Submitted: 27 May 1992 . Accepted: 22 January 1993 . Published Online: 04 June 1998

T. M. Antonsen, and P. Mora

Self-focusing and Raman scattering of laser pulses in tenuous plasmas

T. M. Antonsen, Jr.[a] and P. Mora,
Centre de Physique Théorique, Ecole Polytechnique, 91128 Palaiseau, France

(Received 27 May 1992; accepted 22 January 1993)

The propagation and self-focusing of short, intense laser pulses in a tenuous plasma is studied both analytically and numerically. Specifically, pulses of length of the order of a few plasma wavelengths and of intensity, which is large enough for relativistic self-focusing to occur, are considered. Such pulses are of interest in various laser plasma acceleration schemes. It is found that these pulses are likely to be strongly affected by Raman instabilities. Two different regimes of instability, corresponding to large and small scattering angles, are found to be important. Small-angle scattering is perhaps the most severe since it couples strongly with relativistic self-focusing, leading the pulses to acquire significant axial and transverse structure in a time of the order of the self-focusing time. Thus it will be difficult to propagate smooth self-focused pulses through tenuous plasmas for distances longer than the Rayleigh length, except for pulse duration of the order of the plasma period.

I. INTRODUCTION

There has been considerable recent technological advances of high intensities (of the order of 10^{18} W/cm^2), short pulses lasers (1 psec or less).[1] These lasers could be of great interest in the context of plasma based particle accelerator concepts, in particular for the laser wake field accelerator which uses the ponderomotive force of a short laser pulse to drive an electron plasma wave in a low-density plasma.[2] A severe limitation of the scheme is due to the diffraction of the laser beam. However, it has been argued that self-focusing of the beam could considerably lengthen the interaction region.

If the pulse length τ is much smaller than the inverse of the ion plasma frequency ω_{pi}, the ions' inertia prevents them from moving, and the thermal[3] and usual ponderomotive[4] self-focusing effects are inoperative. However, as pointed out by various authors,[5–7] relativistic self-focusing[8] is relevant in this regime. The laser power is so large that the relativistic corrections to the electron response to the wave field lower the effective plasma frequency thereby increasing the refractive index. In addition, the ponderomotive force tends to expell the electrons from the laser channel, usually enhancing the relativistic effect.

Depending on the laser pulse duration, there exist *a priori* two different regimes for relativistic self-focusing. If the laser pulse duration is much longer than the plasma period, time-independent solutions can be found where the electrons are in equilibrium, the radial ponderomotive force being balanced by the electrostatic force due to charge separation.[6] Such self-focusing occurs when the laser beam power P is above a critical power[5] $P_L = 16.2\ (\omega/\omega_p)^2\ 10^9$ W, where $\omega_p = (4\pi q^2 n_0/m)^{1/2}$ is the plasma frequency based on the ambient density n_0, and q and m are the charge and mass of an electron. Even for rather small values of $(P-P_L)/P_L$, the reduction of the electron density, due to the ponderomotive force expulsion of the electrons, is significant, and this leads to complete expulsion of all electrons within some inner radius for $P > P_c$, where $P_c \approx 1.1\ P_L$ (electron cavitation).[6]

If the laser pulse duration is comparable with the plasma period, the dynamics of the electrons has to be taken into account.[7] As a result, the degree of guiding varies along the pulse. In particular, the forward ponderomotive force pushes the electrons at the front of the pulse leading to an increase of the electron density and this effect tends to exactly cancel the relativistic effect. The front of the pulse then diffracts as a low-intensity beam. These considerations were given by Sprangle *et al.*, on the basis of a one-dimensional analysis of intense laser plasma interactions.[7] Two-dimensional analysis of short laser propagation in tenuous plasmas are usually limited by assumptions on the transverse shape of the laser wave, such as a Gaussian ansatz.[9] The first goal of the present work was to have a correct transverse description of the laser beam during self-focusing and to verify the predictions of Ref. 7.

In addition, there is probably a more fundamental justification of the need for a transverse description of the laser beam. It is well known that high-intensity laser beams are subject to various laser-plasma instabilities.[10–12] The Raman sidescattering is of particular interest here, since it will be found to dominate the pure forward-scattering Raman instability. As a result, a significant part of the laser energy may end up in sidewards scattered waves.[13] We will find two regimes of Raman scattering to be important for finite-size laser pulses. The first regime corresponds to scattering at relatively large angles. Here the instability is spatially convective, and grows either from noise associated with the target plasma or from a seed signal which is part of the angular superposition of waves that compose the incident laser pulse. The instability develops in a relatively short time, namely, the time for the scattered wave to traverse the pulse. The pulse will survive this instability if the number of exponentiations is not too large. The second regime corresponds to scattering at small, but nonzero, forward angles, where there is significant coupling between

[a]Permanent address: Department of Electrical Engineering and Department of Physics, University of Maryland, College Park, Maryland 20742.

 0899-8221/93/051440-13$06.00

the Raman and relativistic self-focusing instabilities. Here the instability is absolute in space, but convective in wave number in a sense that will be described subsequently. The effect of the instability is to cause an incident pulse, which is longer than a plasma wavelength, to acquire axial and transverse structure. According to our estimates and simulations, this structure appears within, roughly, the Rayleigh time for the incident pulse. Thus it will be difficult, if not impossible, to obtain smooth self-focused pulses. These instabilities can affect the propagation of short laser pulses, as we will show in this paper. The second goal of the present work is, therefore, to study the effect of Raman sidescattering on short- and finite-size pulses.

The outline of the paper is follows. In Sec. II we derive the basic equations describing the self-focusing and the Raman sidescattering of ultrashort- and finite-size laser pulses. Section III is devoted to the analysis of the Raman growth. The numerical simulations are described in Sec. IV. A discussion of the results is given in Sec. V.

II. BASIC EQUATIONS

In this section we describe the basic set of equations which govern the propagation of radiation in a tenuous plasma, outline the approximations that are appropriate to the study of self-focusing of the radiation, and address the limitations of these approximations when Raman scattering is important. We start with the equation describing the propagation of the radiation in the limit in which the plasma electron motion is weakly relativistic,

$$\left(\nabla^2-\frac{1}{c^2}\frac{\partial^2}{\partial t^2}\right)\hat{\mathbf{a}}(\mathbf{x},t)=k_p^2\left(1+\frac{\delta n}{n_0}-\frac{1}{2}\langle|\hat{\mathbf{a}}|^2\rangle\right)\hat{\mathbf{a}}(\mathbf{x},t), \tag{1}$$

where $\hat{\mathbf{a}}(\mathbf{x},t)=q\mathbf{A}/(mc^2)$ is the normalized radiation vector potential, and c is the speed of light. The terms on the right-hand side represent the response of the plasma, whose density can be written as the sum of the ambient value, n_0, and a small perturbation δn. The term $\langle|\hat{\mathbf{a}}|^2\rangle$ represents the contribution of the first correction to the relativistic factor $\gamma=1/\sqrt{1-v^2/c^2}$, where $\mathbf{v}=c\,\hat{\mathbf{a}}/\gamma$ is the jitter velocity of an electron in the radiation field. The angular brackets imply an average over the period of time associated with the frequency of the radiation. Finally, the constant $k_p=\omega_p/c$ represents the plasma wave number. Equation (1) is easily derived when the radiation is assumed to be circularly polarized. It is, however, valid for arbitrary polarizations as well.

The density perturbation appearing in Eq. (1) results from the forced excitation of a plasma wave disturbance by the ponderomotive potential of the radiation. In the weakly relativistic limit the density response can be assumed to be linear in the ponderomotive potential, in which case one finds

$$\left(\frac{\partial^2}{\partial t^2}+\omega_p^2\right)\frac{\delta n}{n_0}=c^2\nabla^2\frac{1}{2}\langle|\hat{\mathbf{a}}|^2\rangle, \tag{2}$$

where it has been assumed that the plasma is a cold fluid. Equations (1) and (2) are capable of describing both relativistic self-focusing, as well as stimulated Raman scattering at all angles. It is required that the magnitude of both the normalized vector potential and the relative density perturbation appearing in Eqs. (1) and (2) be small in order that the assumptions of weakly relativistic motion and linear density perturbation remain valid.

In order to investigate self-focusing of a finite duration pulse the para-axial and quasistatic[7] approximations are usually made. The para-axial approximation consists of writing the normalized radiation vector potential as a plane wave propagating in the z direction modulated by a slowly varying three-dimensional envelope

$$\hat{\mathbf{a}}(\mathbf{x},t)=\mathbf{a}(\mathbf{x}_\perp,\xi,t)\exp[i(k_0z-\omega_0t)]+\text{c.c.}, \tag{3}$$

where ω_0 and k_0 satisfy the dispersion relation for plane waves propagating in an unmagnetized plasma, $\omega_0^2=\omega_p^2+k_0^2c^2$, and the variable $\xi=c_gt-z$ measures distance back from the head of the radiation pulse which is moving with a group velocity $c_g=(k_0c^2/\omega_0)$ in the positive z direction. This results in a parabolic equation for the amplitude $\mathbf{a}$

$$\left(2\,i\frac{\omega_0}{c^2}\frac{\partial}{\partial t}+\nabla_\perp^2\right)\mathbf{a}=k_p^2\left(\frac{\delta n}{n_0}-\mathbf{a}\cdot\mathbf{a}^*\right)\mathbf{a}, \tag{4}$$

where we have dropped terms, which are of order ω_p^2/ω_0^2, that are presumed to be small. The quasistatic approximation consists of assuming that the radiation envelope described by Eq. (4) changes little during the time which a plasma electron is within the envelope. In this case, when variables are expressed in terms of t and ξ, one replaces the time derivative in the plasma wave equation (2) according to $\partial/\partial t=c_g\partial/\partial\xi\cong c\partial/\partial\xi$, yielding

$$\left(\frac{\partial^2}{\partial\xi^2}+k_p^2\right)\frac{\delta n}{n_0}=\nabla^2(\mathbf{a}\cdot\mathbf{a}^*). \tag{5}$$

The approximations leading to (4) and (5) are well satisfied if the envelope, $\mathbf{a}$, remains slowly varying and the vector potential and the relative density perturbation remain small. There are two situations, however, under which the assumptions become strained even if they are initially satisfied. The first is the case of strong self-focusing. Solutions of Eqs. (4) and (5) for the case of a laser pulse, which is many plasma wavelengths long, indicate that there is a threshold power for relativistic self-focusing.[5] That is, if the laser power exceeds this threshold it is possible for the laser pulse to adopt a transverse profile that is constant in time and does not diffract. It turns out, however, if this threshold is exceeded by only a small amount, of the order of 10%, then the relative density perturbations become of order unity in the self-guided state and a fully relativistic theory accounting for the nonlinear response of the plasma must be employed.[6]

The second, and perhaps more fundamental problem with Eqs. (4) and (5) is the way in which they treat Raman scattering. In particular, these equations contain what can be described as an ultraviolet catastrophe. Namely, the growth rate for near forward Raman instability is unbounded as the transverse wave number goes to infinity. This divergence is a consequence of having made the para-axial approximation, and does not occur if the full

wave Eq. (1) is solved instead of Eq. (4). In the full equation, the transverse wave number of scattered light is limited by the wavelength of the pump; the maximum scattering angle is 180°. This limitation is not contained in the para-axial approximation. The consequence is that any numerical solution of Eqs. (4) and (5) becomes dependent on the transverse spatial resolution of the variables. The resolution of the problem requires the inclusion of more physics.

It is somewhat surprising that large-angle scattering can be important for the propagation of laser pulses with a finite transverse size. One would expect that disturbances would propagate out of the laser pulse before reaching large amplitude. The problem is that the nonlinear coupling between the radiation and plasma waves that produces the Raman instability increases faster with transverse wave number [due to the Laplacian on the right-hand side of Eq. (2)] than does the transverse group velocity of the scattered radiation. Thus perturbations grow as they convect out of the pump. As we will show in the next section where we treat the Raman problem analytically, both for systems (1), (2), (4), and (5), the number of exponentiations of a scattered wave is an increasing function of the scattering angle. The maximum number of exponentiations is then determined by whatever physics limits the maximum transverse wave number. The practical consequence of the instability is that the trailing end of a laser pulse for which the maximum number of exponentiations is too large will blow apart.

In spite of the foregoing discussion, the para-axial equation (4), can still be used to analyze the propagation of laser pulses in tenuous plasmas. We will argue that to the extent that the additional physics, not contained in the para-axial equation, leads to an upper limit on the transverse wave number of the scattered light, this physics can be modeled by solving the para-axial equation with a controlled transverse spatial resolution. In Sec. IV we will present such solutions, illustrating the effect of the Raman instability for the case in which the governing equations are solved via a finite difference scheme on a two-dimensional grid. In this case a certain degree of care must be exercised in controlling the shortest allowed wavelengths as will be discussed. Finally, Sec. V will contain our conclusions and will outline some of the remaining questions regarding light propagation in tenuous plasmas.

III. ANALYSIS OF RAMAN GROWTH IN FINITE-SIZE PULSES

In this section we consider the growth of the Raman instability as it affects the propagation of finite-sized laser pulses. It will be found that the instability is of a convective nature. Thus a precise calculation of the threshold would, in principle, involve details of the shape of the laser pulse (the pump), as well as the level of noise from which the instability is to grow. Such a theory is not easily carried out since the shape of the laser pulse is continually changing as it propagates, and the level of noise can depend on effects not always contained in the basic equations. An additional consideration of a more fundamental nature is the fact that for near forward scattering it is not possible to make a formal distinction between the equilibrium state and the small perturbation whose linear growth is to be determined. This is because the finite size of the radiation pulse implies that the "equilibrium," or pump, already contains the wave vectors that will be considered as the "perturbation." As a result, when precise answers are required, the best course of action is to simulate the full governing equations that describe simultaneously the evolution of pump and the perturbation. The results of such simulations will be presented in the next section. In this section, we will present estimates of the amount of growth that can be expected, based on the dispersion relation which applies to the case of an infinite homogeneous pump. The finite size of the pump is treated by using the local dispersion relation to calculate the space- and time-dependent impulse response for the system. In this way the amount of growth a perturbation experiences before it encounters the boundary of the pump can be estimated. Two different regimes of Raman growth, which correspond to relatively large and small scattering angles, are found to be important. As will be indicated, these regimes require separate treatment. The estimates will then give basic scaling relations for the growth of scattered radiation which will be compared with the more detailed simulations.

We now outline the derivation of the dispersion relation which determines the stability of an infinite homogeneous pump as described by Eqs. (1) and (2). The resulting dispersion relation, already derived by McKinstrie and Bingham,[11] is a generalization, to the case in which relativistic self-focusing is important, of the standard dispersion relation describing the coupling of high- and low-frequency waves in a plasma.[10] Here, due to the assumption of a tenuous plasma, we treat plasma waves as being low frequency, and assume the ions are stationary. The radiation field will be assumed to be plane polarized and consist of a pump of amplitude a_0 and two daughter waves a_+ and a_- propagating at an angle to the pump,

$$\begin{aligned}\hat{\mathbf{a}}(\mathbf{x},t)=\mathbf{e}_p\{&a_0+a_+\exp[i(\mathbf{k}\cdot\mathbf{x}-\omega t)]\\&+a_-\exp[-i(\mathbf{k}\cdot\mathbf{x}-\omega^* t)]\}\\&\times\exp[i(k_0 z-\omega_0 t)]+\text{c.c.},\end{aligned}\tag{6}$$

where $\mathbf{e}_p$ is a unit vector giving the direction of polarization, $\mathbf{k}$ and ω are the wave number and frequency shift of the scattered radiation, $\mathbf{e}_p\cdot\mathbf{k}=\mathbf{e}_p\cdot\mathbf{e}_z=0$, and ω_0 and k_0 satisfy the dispersion relation $\omega_0^2=\omega_p^2(1-a_0^2)+k_0^2c^2$. The beating of the pump and scattered waves gives rise to a time- and space-dependent ponderomotive potential which, to first order in the amplitudes of the scattered waves, is

$$\tfrac{1}{2}\langle|\hat{\mathbf{a}}|^2\rangle=a_0^2+\{(a_++a_-^*)a_0\exp[i(\mathbf{k}\cdot\mathbf{x}-\omega t)]+\text{c.c.}\}.\tag{7}$$

This, in turn, drives an electron density perturbation of the form

$$\frac{\delta n}{n_0}=\eta\exp[i(\mathbf{k}\cdot\mathbf{x}-\omega t)]+\text{c.c.}\tag{8}$$

Inserting the preceding expressions for the dependent variables in Eqs. (1) and (2), and combining the equations' results in the dispersion relation

$$(\omega^2-\omega_p^2)\left(\frac{D_+D_-}{D_++D_-}+a_0^2\omega_p^2\right)=a_0^2\omega_p^2c^2k^2, \tag{9}$$

where the quantities D_+ and D_- are the dispersion relations for the scattered waves in the absence of plasma density fluctuations,

$$D_\pm=(\omega_0\pm\omega)^2-(k_0\pm k_z)^2c^2-k_\perp^2\,c^2-\omega_p^2(1-a_0^2). \tag{10}$$

Here, k_z and $k_\perp$ are the components of the wave vector $\mathbf{k}$.

The dispersion relation (9) describes the interaction of the relativistic modulational instability (self-focusing) with the Raman instability at arbitrary angles for the case of a cold electron fluid. Solutions of this dispersion relation describing the interaction of these instabilities have been discussed extensively by McKinstrie and Bingham.[11] In the case in which the quasistatic and para-axial approximations are made, one effectively transforms to a frame moving with the pump pulse. The quasistatic assumption leads to the replacement of ω appearing in the plasma wave dispersion relation in (9) by k_zc. The para-axial approximation leads to the expansion of the daughter wave dispersion relations for $k_z\ll k_0$,

$$D_\pm=\pm2\omega_0\omega_1-k_\perp^2\,c^2,$$

where $\omega_1=\omega-k_zc_g=\omega-k_zc$. A detailed comparison of the various regimes of Raman scattering in the infinite, homogeneous pump limit for the two dispersion relations [the full dispersion relation (9) and the quasistatic/para-axial dispersion relation] is presented in Appendix A.

A. Large-angle scattering

We will focus on the Raman instability for propagation angles which are not too small. In particular, we write the wave vector $\mathbf{k}$ as the sum of a zero-order part which is chosen to satisfy the dispersion relation $D_-(\omega=0,k_0\mathbf{e}_z-\mathbf{k})=0$, plus a small correction $\delta\mathbf{k}$,

$$k_\perp=-\sin\theta\,k_0+\delta k_\perp\,,$$

$$k_z=(1-\cos\theta)k_0+\delta k_z\,.$$

Here θ is the angle of propagation, with respect to the z axis of the scattered wave whose frequency is approximately ω_0. We then assume the frequency ω and wave number $\delta\mathbf{k}$ are small and Taylor expand D_- obtaining

$$D_-\approx-2\omega_0[\omega-c_g(\cos\theta\,\delta k_z+\sin\theta\,\delta k_\perp)].$$

The quantity D_+ is approximated as

$$D_+\approx4k_0^2\,c^2(\cos\theta-1),$$

and we assume $D_+\gg D_-$. This last assumption will be justified when the growth rate we are about to find is small enough so that $|\omega/\omega_0|\ll(1-\cos\theta)$. Thus, essentially, we are neglecting the anti-Stokes sideband, which is permissible provided the scattering angle is large enough.[11,14]

Inserting the expression for D_- into Eq. (9), using $D_-\ll D_+$, and ignoring the relativistic self-focusing term $a_0^2\omega_p^2$ on the left-hand side (actually, this term could be removed by an appropriate shift of the wave number $\delta\mathbf{k}$), we arrive at the cubic dispersion relation

$$D(\omega,\delta\mathbf{k})=0, \tag{11}$$

where

$$D(\omega,\delta\mathbf{k})=(\omega^2-\omega_p^2)[\omega-c_g(\cos\theta\,\delta k_z+\sin\theta\,\delta k_\perp)]+\omega_c^3, \tag{12}$$

and

$$\omega_c^3=\frac{2a_0^2\omega_p^2c^2k_0^2}{\omega_0}\sin^2\left(\frac{\theta}{2}\right), \tag{13}$$

is the coefficient of coupling between the scattered wave and the plasma density perturbation. Note that this coupling frequency vanishes for forward scattering, $\theta=0$, and increases progressively with scattering angle reaching a maximum for backscattering, $\theta=\pi$. In an infinite homogeneous pump, where one is free to specify the wave number $\mathbf{k}$, and hence $\delta\mathbf{k}$, dispersion relation (11) predicts unstable solutions with temporal growth rates. The scaling of these solutions depends on whether the coupling frequency ω_c is greater or smaller than the plasma frequency. When the coupling frequency is much greater than the plasma frequency one is in the Compton regime and one finds the complex frequency at maximum growth rate to be given by

$$\omega=\frac{\omega_c}{2}(\sqrt{3}\,i+1).$$

In the opposite limit where the coupling frequency is less than the plasma frequency, one is in the Raman regime and the frequency at maximum growth rate satisfies

$$\omega=\omega_p\left[\frac{i}{\sqrt{2}}\left(\frac{\omega_c}{\omega_p}\right)^{3/2}+1\right].$$

Note that the frequency of the scattered wave is down shifted in both cases as it should be.

We are not interested in the temporal growth rate of disturbances which are infinitely extended. Rather, we wish to assess the amount of growth than can be expected when the region of the pump is of finite size. To do this we use the method of determination of the impulse response due to a localized disturbance at $\mathbf{x}=0$ and $t=0$, implied by Eq. (11), as described by Bers.[15] Specifically, we define a shifted frequency $\omega'=\omega-\delta\mathbf{k}\cdot\mathbf{v}$ and a shifted dispersion function

$$D_v(\omega',\delta\mathbf{k})=D(\omega'+\delta\mathbf{k}\cdot\mathbf{v},\delta\mathbf{k}),$$

where $\mathbf{v}=\mathbf{x}/t$, and solve simultaneously the equations $D_v=0$, and $\partial D_v/\partial\delta\mathbf{k}=0$. The quantity $\mathrm{Im}\{\omega't\}$ then gives the number of exponentiations experienced by the disturbance as observed at the point $\mathbf{x}$ at time t.

Solution of the equation, $\partial D_v/\partial\delta\mathbf{k}=0$, yields two results. First, one finds that the velocity $\mathbf{v}=\mathbf{x}/t$ must be parallel to the group velocity of the scattered radiation whose components are $c_g\cos\theta$ and $c_g\sin\theta$ in the directions parallel and perpendicular to the direction of propagation of the pump. Physically, this implies that the disturbance will

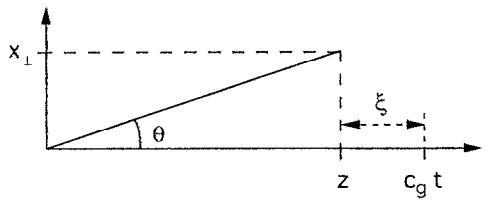

FIG. 1. Geometry for the scattered light.

be localized along the trajectory of the scattered electromagnetic wave. Second, one obtains a relation between $\omega=\omega'+\delta\mathbf{k}\cdot\mathbf{v}$ and $\delta\mathbf{k}$,

$$[\omega-c_g(\cos\theta\,\delta k_z+\sin\theta\,\delta k_\perp)]=\left(\frac{1-\beta}{\beta}\right)\frac{(\omega^2-\omega_p^2)}{2\omega}, \tag{14}$$

where $\beta=|\mathbf{x}|/c_g t$. Substitution of (14) into the dispersion relations (11) and (12) then determines the frequency ω,

$$\left(\frac{1-\beta}{\beta}\right)\frac{(\omega^2-\omega_p^2)^2}{2\omega}=-\omega_c^3. \tag{15}$$

The number of exponentiations of the disturbance as it propagates is then obtained by inserting the solution of (15) into the definition of ω' and using (14) to eliminate $\delta\mathbf{k}$,

$$\mathrm{Im}\{\omega' t\}=t(1-\beta)\,\mathrm{Im}\left\{\omega+\frac{\omega^2-\omega_p^2}{2\omega}\right\}. \tag{16}$$

Expression (16) thus gives the amount of growth that would be experienced by a disturbance, initiated at the origin at $t=0$, as it propagates along the characteristic of a scattered wave making an angle θ, with respect to the direction of propagation of the pump.

Our concern is the amount of exponentiation a disturbance experiences before it leaves the region of the pump. Thus we would like to characterize (16) in terms of variables which measure the location of the disturbance in the moving pump pulse. The position of a point in the pump pulse is determined by its transverse coordinate $x_\perp$, and the distance back from the head of the pulse $\xi=c_g t-z$. The relation between these variables and the lab frame quantities $|\mathbf{x}|$, θ, and t, is illustrated in Fig. 1. Using simple trigonometric relations, one finds the time for a disturbance to propagate from the center of the head of the pulse $x_\perp=0$, $\xi=0$, to the point $(x_\perp,\xi)$ is given by

$$c_g t=\xi+x_\perp\cot\theta,$$

provided this is a positive number. The quantity $\beta=|\mathbf{x}|/c_g t$ appearing in (16) can also be expressed in terms of these coordinates,

$$\beta=\frac{x_\perp}{\xi|\sin\theta|+x_\perp\cos\theta}.$$

This latter relation restricts the angle θ such that for given values of ξ and $x_\perp$, β is less than unity.

The procedure now is to insert the expressions for β and t into (15) and (16) and arrive at the amount of exponentiation. The solution of (15) depends on a single parameter,

$$R=\left(\frac{\omega_c}{\omega_p}\right)^3\left(\frac{\beta}{1-\beta}\right).$$

For $R\gg 1$, one is in the Compton regime and (15) yields

$$\omega=\frac{\omega_c}{2^{2/3}}(\sqrt{3}i+1)\left(\frac{\beta}{1-\beta}\right)^{1/3}.$$

The amount of exponentiation is then found from (16) to be

$$\mathrm{Im}\{\omega' t\}=\kappa_c|x_\perp|^{1/3}|\xi-|\tan\frac{\theta}{2}|x_\perp|^{2/3}, \tag{17}$$

where the effective spatial growth rate in the Compton regime is given by

$$\kappa_c=\frac{3^{3/2}}{4}\left\{2a_0^2k_p^2k_0\left|\tan\frac{\theta}{2}\right|\right\}^{1/3}, \tag{18}$$

and we have assumed $c_g=c$. For $R\ll 1$, one is in the Raman regime and (15) yields

$$\omega=\omega_p\left\{\frac{i}{2}\left(\frac{2\beta\omega_c^3}{(1-\beta)\omega_p^3}\right)^{1/2}+1\right\},$$

for which case the amount of exponentiation is found to be

$$\mathrm{Im}\{\omega' t\}=\kappa_r|x_\perp|^{1/2}|\xi-|\tan\frac{\theta}{2}|x_\perp|^{1/2}, \tag{19}$$

where the effective spatial growth rate in the Raman regime is given by

$$\kappa_r=\left\{2a_0^2k_pk_0\left|\tan\frac{\theta}{2}\right|\right\}^{1/2}. \tag{20}$$

It is interesting to note that, due to the appearance of the quantity β in (15), whether the Raman or Compton regime pertains depends not only on the intrinsic parameters such as the plasma and coupling frequencies, but also on where and at what time the disturbance is examined. If one is close to the front of the propagating disturbance, $\beta\cong 1$, then the Compton regime applies even if coupling frequency is less than the plasma frequency. This is due to the fact that as the disturbance enters a new, undisturbed region of plasma, the growth of the density fluctuations is limited at first by the inertia of the electrons, as opposed to the built-up electrostatic field. Thus one can ignore the plasma frequency appearing in Eq. (2) compared with the time derivative. Note, however, from (16), the amount of exponentiation will be small close to the front of the disturbance.

We now examine the dependence of the amount of exponentiation on the coordinates within the pulse and the angle of propagation. To do this we focus on the Raman expressions given by (19) and (20). It is clear from (19) that the larger the value of ξ, the greater the exponentiation. Thus to estimate the maximum expected growth, we

insert for ξ the length of the pulse L. The dependence of the growth on the transverse coordinate is such that there is a maximum growth occurring for

$$x_\perp = \frac{L}{2\,|\tan(\theta/2)|}. \tag{21}$$

Whether this point is within the pulse depends on the angle θ. If W is the width of the pulse then the maximum will lie within the pulse provided that the scattering angle exceeds a critical value obtained by replacing $x_\perp$ by W in the above. For angles greater than this critical angle, we insert (21) and (20) into (19) and obtain an expression for the amount of growth which, surprisingly, is independent of angle

$$\mathrm{Im}\{\omega' t\} = L\left(\frac{a_0^2 k_p k_0}{2}\right)^{1/2}. \tag{22}$$

Thus for angles greater than the critical angle, the amount of growth is the same as for pure backscatter. For angles less than the critical angle the amount of growth is obtained from (19) and (20) by inserting the length of the pulse, L, for ξ and the width of the pulse, W, for $x_\perp$. As a function of angle, the amount of growth increases monotonically until the critical angle is reached after which it is constant. Similar conclusions are reached in the Compton regime.

It is now instructive to ask: What is the amount of growth expected from the simplified set of equations (4) and (5)? This can be obtained from (17)–(20) by letting $\theta \approx k_\perp / k_0$ be small. The results are

$$\mathrm{Im}\{\omega' t\} = \frac{3^{3/2}}{4}\,|x_\perp|^{1/3}|\xi|^{2/3}(a_0^2 k_p^2 k_\perp)^{1/3} \tag{23a}$$

and

$$\mathrm{Im}\{\omega' t\} = |x_\perp|^{1/2}|\xi|^{1/2}(a_0^2 k_p k_\perp)^{1/2} \tag{23b}$$

in the Compton and Raman regimes, respectively. Thus in both cases the number of exponentiations increase with perpendicular wave number, without limit. Thus without any restriction on the perpendicular wave number, the simplified set of equations is poorly posed in the sense that the results are dependent on the resolution with which the equations are solved.

A more severe problem affects numerical solutions of (4) and (5) in which the transverse dependence of the field variables is based on a finite difference scheme. This can be understood by first considering the situation in which we suppose the pump wave is infinitely extended in the transverse direction and ignore the convection of the disturbance in that direction. That is, suppose we set $\delta k_\perp$ to zero in (12) and resolve the impulse propagation problem. The results can be obtained from (23a) and (23b) by substitution of $ck_\perp t/k_0$ for $x_\perp$. That is, by expressing $x_\perp$ in terms of the time required for the disturbance to reach that point. The result is that for fixed ξ any disturbance eventually diverges with time. That is, the instability changes from convective to absolute in nature. This is of significance to finite difference simulations because the continuous wave number $k_\perp$ is replaced in the finite difference system by $2\sin(k_\perp\, dx/2)/dx$, where dx is the spacing of the grid. Thus the numerical group velocity in the transverse direction $[v_g = c\sin(k_\perp\, dx)/(k_0\, dx)]$ vanishes for the shortest wavelength disturbance, $k_\perp\, dx = \pi$, and the instability is absolute. In the next section we will discuss a way of suppressing this problem by carefully controlling the maximum spatial wave number.

Finally, since the instability is convective, we must discuss the source, or seed, signal which is to be amplified. There are a number of possible sources that can produce signals which will subsequently grow as the pulse propagates. The first of these that comes to mind is the spontaneous noise associated with the discreteness of the plasma electrons' charge. This noise excites plasma waves which reach a level that can be estimated by attributing an amount of energy equal to the plasma temperature to each mode in k space

$$\left\langle \left(\frac{\delta n}{n_0}\right)^2 \right\rangle = \int \frac{d^3k}{(2\pi)^3}\frac{k^2 T}{m n_0 \omega_p^2},$$

where the integral is cut off for wavelengths shorter than the Debye length. Not all modes in k space will be resonant with the pump and decay waves which lead to a reduction in the noise level available to excite the instability. We estimate this reduction by restricting the integral in the above to a spherical shell in k space with a radius equal to the wave number of the pump and a thickness proportional to the spatial growth rate of the convective instability. This produces the following estimate for the level of noise in plasma waves that is to be amplified,

$$\left\langle \left(\frac{\delta n}{n_0}\right)^2 \right\rangle_{\mathrm{eff}} = \frac{4\pi\gamma_e k_0^2 \lambda_d^2}{\omega_0 N_*},$$

where γ_e is the effective temporal growth rate, λ_d is the Debye length, and $N_* = n_0\lambda_0^3$ is the number of electrons in a cube of side $\lambda_0 = 2\pi/k_0$. This is just a rough estimate, and a more detailed calculation, which includes the k dependence of the amount of exponentiation, should be carried out. It is likely that such a calculation would reveal that backscattered radiation is most easily excited by this type of noise. We will assume that the level of this noise is extremely small, and since the focus of this paper is on near forward scattering, we will leave this issue to future studies.

A second source of signal which can be amplified is determined by the initial shape of the radiation pulse as it enters the plasma. For a pulse with a true Gaussian shape, the transverse Fourier spectrum falls off exponentially with the transverse wave number. However, a pulse that has been passed through an aperture will have a high wave-number tail that falls algebraically with wave number. Given that the amount of exponentiation of scattered radiation increases with transverse wave number, such apertured beams will contain high wave-number components that will initially be amplified before leaving the pulse. If the amount of amplification is large enough a significant

fraction of the radiation in the pulse can be scattered. This effect will be illustrated in the numerical simulations presented in the next section.

B. Small-angle scattering

We now consider the problem of near forward scattering. Here it is not possible to make a formal distinction between the pump and the scattered radiation due to the finite size of the pump pulse. In this case, the slow evolution of the pulse due to diffraction can serve as a seed for exciting plasma waves and slightly scattered radiation. Our simulations reveal an effect which we interpret in this way. Namely, the Gaussian-shaped pulse acquires a perturbation with an axial wavelength equal to the plasma wavelength and a transverse structure which appears to be a Gaussian modulated by a sine wave with a wavelength comparable to the width of the pulse. We consider this case analytically by returning to dispersion relation (9). For near forward scattering, we assume the axial wave number is small compared to the laser wave number, $k_z \ll k_0$, and we approximate the daughter dispersion relations $D_{\pm}$, according to

$$D_{+} = \pm 2\omega_0\omega_1 - k_{\perp}^2 c^2,$$

where

$$\omega_1 = \omega - ck_z .$$

Here, we have replaced the group velocity c_g by the speed of light. We assume that the perturbations that develop satisfy the quasistatic approximation, and we replace ω in the plasma-wave dispersion relation by ck_z. With these approximations Eq. (9) reduces to $D(\omega_1,\mathbf{k})=0$, where

$$D(\omega_1,\mathbf{k}) = \left(\frac{2\omega_1\omega_0}{c^2}\right)^2 - k_{\perp}^4 - 2k_{\perp}^2 \frac{a_0^2 k_p^2 (k_p^2 + k_{\perp}^2)}{(k_z^2 - k_p^2)} . \tag{24}$$

This dispersion relation describes both the relativistic self-focusing instability, as well as the near forward Raman instability when both the Stokes and anti-Stokes scattered waves are important. Further, it represents the dispersion relation that one obtains upon linearization of the paraxial, quasistatic equations, and as such it describes perturbations in the frame of the moving pulse. For disturbances whose transverse wavelength is longer than the plasma wavelength we may neglect $k_{\perp}^2$ compared with k_p^2 in the parentheses in the numerator of the above. The opposite limit, namely $k_{\perp}^2 \gg k_p^2$, leads to (23a) and (23b) which we have already discussed.

We now determine the impulse response as before. Specifically, we define $\omega' = \omega_1 - \mathbf{k}\cdot\mathbf{v}$ and the shifted dispersion relation $D_v(\omega',\mathbf{k}) = D(\omega' + \mathbf{k}\cdot\mathbf{v},\mathbf{k})$ and solve simultaneously the equations $D_v = 0$ and $dD_v/d\mathbf{k} = 0$. As the resulting instability is absolute, in so far as its propagation in the perpendicular direction is concerned, we set the perpendicular part of the velocity $\mathbf{v}$ equal to zero. The vanishing of the derivative of the dispersion function (24), with respect to the perpendicular component of the wave vector, then determines the perpendicular component of the wave vector,

$$k_{\perp}^2 = -\frac{a_0^2 k_p^4}{(k_z^2 - k_p^2)} . \tag{25}$$

Inserting this relation in the derivative, with respect to k_z of the dispersion function (24), then gives

$$\frac{\partial D_v(\omega',\mathbf{k})}{\partial k_z} = \left(\frac{2\omega_1\omega_0}{c^2}\right)\frac{4\omega_0 v_z}{c^2} - \frac{4k_z(a_0^2 k_p^4)^2}{(k_z^2 - k_p^2)^3} = 0. \tag{26}$$

And, inserting the expression for the perpendicular wave number (25) into the dispersion relation (24) allows one to calculate the frequency ω_1,

$$\left(\frac{2\omega_1\omega_0}{c^2}\right) = i\sigma \frac{a_0^2 k_p^4}{(k_z^2 - k_p^2)} , \tag{27}$$

where σ is plus or minus one. Combining (26) and (27) to eliminate ω_1 then determines the axial wave number

$$\frac{(k_z^2 - k_p^2)^2}{k_z} = i\sigma \frac{a_0^2 k_p^4 c^2 t}{\omega_0 \xi} , \tag{28}$$

where we have replaced v_z by $-\xi/t$. The above is similar to our other dispersion relations in that it has both a Raman and a Compton limit. In this case, for fixed ξ, the Raman limit applies for early times, and the Compton limit applies for later times. The transition occurs at a critical time t_c which is given by

$$t_c = T_R \frac{2k_p\xi}{k_p^2 R^2 a_0^2} ,$$

where

$$T_R = \frac{R^2\omega_0}{2c^2}$$

is the Rayleigh time for a pulse of width R, and $k_p^2 R^2 a_0^2$ is essentially the peak power in the pulse normalized to the critical value for self-focusing. Thus the transition time, measured in units of the Rayleigh time, depends on the length of the pulse, as measured in plasma wavelengths, and the instantaneous power of the pulse, as measured in units of the critical power for self-focusing. For our simulations to be presented in the next section, the Raman regime result is relevant.

Before calculating the amount of exponentiation, it is interesting to examine the behavior of the perpendicular wave number with time. For early times (28) shows that k_z is close to k_p and the perpendicular wave number determined by (25) is large. As time progresses, the perpendicular wave number decreases. The present calculation applies only so long as the predicted perpendicular wave length is smaller than the transverse size of the pulse. Once this inequality is violated a different rate of growth will obtain. In this sense the instability is convective in k space.

At the critical time, when k_z is of the order of k_p we have

$$k_{\perp}^2 R^2 \simeq a_0^2 k_p^2 R^2 .$$

Thus at the critical time the perpendicular wavelength is the same as one would obtain for the relativistic self-focusing instability. Further, for power levels below the

self-focusing threshold the perpendicular wavelength predicted by the infinite, homogeneous medium theory is larger than the transverse size of the pulse. For this reason the Compton regime is probably difficult to realize.

We now estimate the amount of exponentiation for the impulse response. That is, we calculate

$$\mathrm{Im}\{\omega' t\}=\mathrm{Im}\{\omega t+k_z\xi\}=k_p\xi\ \mathrm{Im}\left\{i\sigma\frac{k_p^2}{2(k_z^2-k_p^2)}\frac{t}{t_c}+\frac{k_z}{k_p}\right\}.$$

At the critical time, this is of the order of the length of the pulse measured in plasma wavelengths. For times less than the critical time we have from (28)

$$k_z=k_p\left[1+\left(\frac{i\sigma t}{4t_c}\right)^{1/2}\right].$$

This gives the following estimate for the amount of exponentiation,

$$\mathrm{Im}\{\omega' t\}=k_p\xi\left(\frac{t}{2t_c}\right)^{1/2}=\left(\frac{a_0^2k_p\xi\omega_p^2t}{2\omega_0}\right)^{1/2}. \tag{29}$$

Thus long pulses, with $k_pL\gg 1$, will eventually loose their smooth shape and develop transverse and axial structure. The amount of time required for this structure to appear can be estimated from the above by setting the amount of exponentiation to unity and solving for t,

$$t=4T_R/(k_pLa_0^2k_p^2R^2).$$

Thus for pulses at or above the threshold for self-focusing, and which are longer than a plasma wavelength, the structure will appear on the order of a Rayleigh time. Since, as shown by Sprangle *et al.*,[7] the pulse must be longer than a plasma period to self-focus at all, we anticipate that it will be very difficult to produce a smooth, self-focused laser pulse.

IV. NUMERICAL SIMULATIONS

We now describe the results of numerical simulations of the propagation of laser pulses through plasmas. We adopted the simplified set of equations (4) and (5) and wrote a finite difference algorithm for their solution on a two dimensional Cartesian grid (ξ,x). The radiation was assumed to be plane polarized with complex amplitude $a(\xi,x,t)$ in the direction perpendicular to the plane of the simulation. We introduced the variable

$$\chi=\frac{\delta n}{n_0}-|a|^2$$

to represent the perturbed index of refraction. This allows (4) and (5) to be rewritten

$$\left(2i\frac{\omega_0}{c^2}\frac{\partial}{\partial t}+\frac{\partial^2}{\partial x^2}\right)a=k_p^2\chi a, \tag{30a}$$

$$\left(\frac{\partial^2}{\partial\xi^2}+k_p^2\right)\chi=\left(\frac{\partial^2}{\partial x^2}-k_p^2\right)|a|^2. \tag{30b}$$

This system can then be differenced in time in a completely implicit way, wherein (30a) is centered between two time levels and (30b) solved at each time level. Evaluating the nonlinear term on the right-hand side of (30a) as the product of the time centered index of refraction and the time centered field then gives the finite difference equations the property of exact energy conservation.

The following boundary conditions were imposed on the finite difference equations. Equation (30b) was integrated in ξ assuming that both χ and its derivative vanished upstream from the laser pulse ($\xi<0$). The field variable a was assumed to possess even symmetry in x and to satisfy outgoing wave-boundary conditions at $x=X_{\max}$. The outgoing wave-boundary conditions were enforced by a method which is described in Appendix B. Outgoing boundary conditions are important for long simulation runs because of the convective nature of the Raman instability. The most convectively unstable disturbances have the largest perpendicular wavelengths and hence, the highest group velocities in the x direction. If these disturbances are reflected at the simulation boundary back into the laser pulse, then the convective character of the instability can be changed to absolute. Finally, the radiation profile as a function of ξ and x was specified. Typically, the axial profile was chosen to be of the form of a half-sine wave, and the radial profile was chosen to be a converging Gaussian beam.

As has been mentioned, in a straightforward finite differencing scheme as we have described, the continuous wave vector $k_\perp$ is replaced by $2\sin(k_\perp\,dx/2)/dx$, and the group velocity for perturbations with the maximum wave number vanishes giving rise to absolute instability. To eliminate this problem we filtered the wave function $a(\xi,x,t)$ periodically during the course of a simulation. The filter worked by smoothing the field over a range of nine transverse grid points

$$a'(x_i)=a(x_i)-\sum_{j=1}^{4}\frac{1}{2}c_j[a(x_{i+j})+a(x_{i-j})-2a(x_i)],$$

where $a'(x_i)$ is the filtered field. The coefficients c_j were chosen, such that the transfer function,

$$T(k_\perp)=1-\sum_{j=1}^{4}c_j[\cos(jk_\perp\,dx)-1],$$

was unity to order $k_\perp{}^8$ at long wavelengths and zero when $k_\perp=\pi/dx$, where dx is the spacing of the grid in x. The resulting transfer function is plotted in Fig. 2. The frequency of application of the filter was then specified so as to suppress any instability with $k_\perp\,dx>0.8\pi$. In doing this we assumed that the convective growth of the instability was given by Eq. (23b). A test of the efficiency of the filter was the degree to which energy remained conserved. As mentioned, the basic finite difference scheme conserves energy exactly (except for round-off error). This is no longer true when the filter is added. However, if the filter is working properly, that is if the transfer function is sharp enough, then it will act only to suppress the instability and energy will be conserved to a high degree of accuracy.

The results of several simulations in the form of pseudo-three-dimensional plots of the square of the nor-

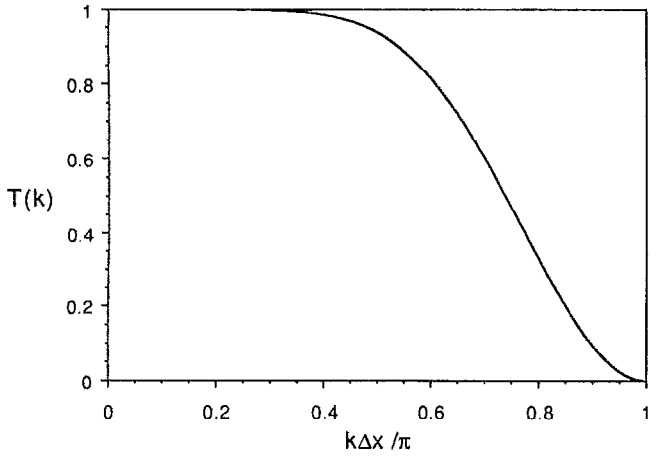

FIG. 2. Transfer function specified so as to suppress the instability with $k_\perp\, dx > 0.8\pi$.

malized vector potential are shown in Figs. 3(a)–3(c). The initial radiation pulse had the form

$$a(x,\xi,t=0)=a_0 \sin(\pi\xi/L)\exp(-x^2/R^2) \times[1+\cos(\pi x/X_{\max})]/2, \quad (31)$$

where for the plots of Figs. 3(a) and 3(b) the relevant parameters are $a_0=0.32$, $k_pL=80$, $k_pR=16$, and $k_pX_{\max}=32$. The last factor in (31) ensures that, initially, the vector potential and its radial derivative vanish at the boundary. This reduces the high k components that would be present if the initial vector potential was simply cut off at the boundary. The numerical resolution for the simulations were as follows: 81 grid points were used in the axial direction and 122 grid points were used in the radial direction for the cases of Figs. 3(a) and 3(b), and 62 grid points were used for the case of Fig. 3(c).

Figure 3(a) shows the field intensity at a time equal to 0.35 times the Rayleigh time, based on the width R, viz., $t=0.35\ T_R$, where $T_R=0.5\ \omega_0\ R^2/c^2$. One can see the development of the scattered radiation on the trailing end of the pulse. The axial wavelength of the perturbations is equal to the plasma wavelength, and radial wavelength is equal to the shortest value allowed by the filter. Increasing the radial resolution results in finer scale perturbations. This radiation has grown from the high k components of the initial waveform, which are present due to its finite radial extent.

Figure 3(b) shows a continuation of the same simulation now at one-half the Rayleigh time. Several important features are visible. First, the body of the pulse has self-focused to a high degree. As predicted by Sprangle *et al.*,[7] the head of the pulse has not focused. The high perpendicular radial wave-number scattered radiation is still visible at the very end of the pulse, but its magnitude has diminished slightly from that in Fig. 3(a). A new perturbation is seen to develop in the body of the pulse. The axial wave-

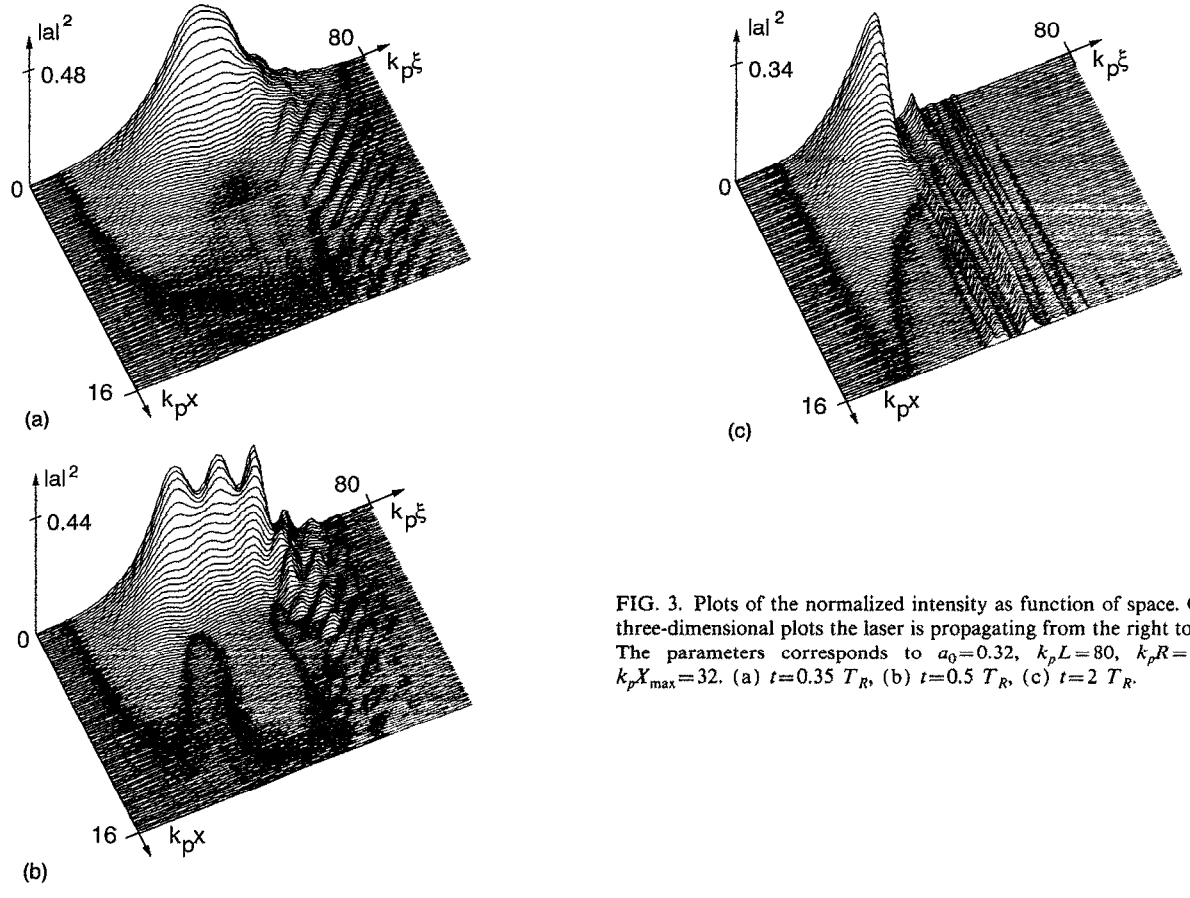

FIG. 3. Plots of the normalized intensity as function of space. On these three-dimensional plots the laser is propagating from the right to the left. The parameters corresponds to $a_0=0.32$, $k_pL=80$, $k_pR=16$, and $k_pX_{\max}=32$. (a) $t=0.35\ T_R$, (b) $t=0.5\ T_R$, (c) $t=2\ T_R$.

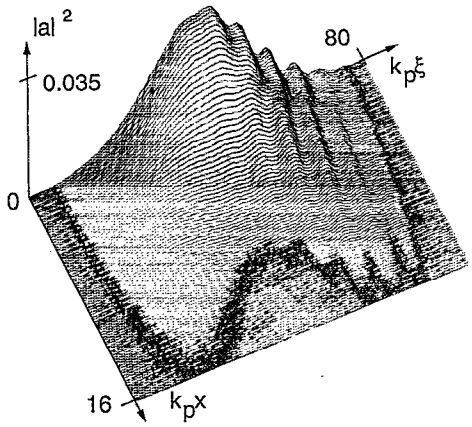

FIG. 4. Same as Fig. 3 for a lower intensity. Parameters are $a_0=0.16$, $k_pL=80$, $k_pR=16$, $k_pX_{max}=128$, and $t=2\ T_R$.

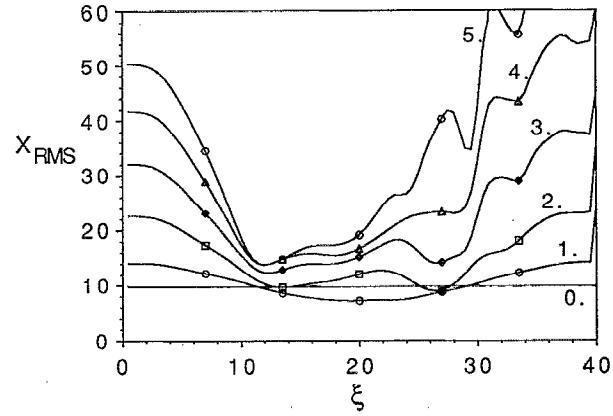

FIG. 5. Root-mean-squared width of the pulse as a function of the axial distance for $t=0$ to 5 T_R. Parameters are $a_0=0.16$, $k_pL=40$, $k_pR=20$, and $k_pX_{max}=160$.

length of the perturbation is, again, the plasma wavelength but the radial wavelength is larger than that of the perturbation at the tail of the pulse. In order to ascertain the effects of this perturbation we reduced the radial resolution by a factor of 2 and simulated the pulse for a much longer time. The result appears in Fig. 3(c) which shows the shape of the pulse at 2.0 Rayleigh times. The tail of the pulse has now been completely eroded by scattering. The degree of scattering is dramatic due to our choice of a rather large initial normalized field amplitude. Due to the relatively long radial wavelength of the scattered radiation in this case, we interpret this instability as being the coupled Raman self-focusing branch studied in the previous section. This scattering is an inherent feature of intense pulse propagation in tenuous plasmas.

To illustrate the dependence of these instabilities on radiation amplitude we simulated a weaker pulse. Figure 4 shows the result, at 2.0 Rayleigh times, of a simulation in which the initial amplitude has been reduced to $a_0=0.16$. Because of the reduction of the field amplitude, there is considerably less self-focusing. As a result, we increased the radial size of the simulation region to $k_pX_{max}=128$. The number of radial grid points used in this case was 242. Here, the long perpendicular wavelength instability is visible on the trailing end of the pulse.

Figure 5 illustrates the degree of self-focusing present for a simulation with the following parameters, $a_0=0.16$, $k_pL=40$, $k_pR=20$, and $k_pX_{max}=160$. Plotted is the root-mean-squared width of the pulse as a function of axial distance for several different times. As predicted,[7] the head of the pulse expands in time, due to diffraction, just as it would in the absence of any guiding. The body of the pulse remains focused for the duration of the simulation. There is, however, considerable excitation of the Raman instability, as evidenced by the appearance of oscillations on the tail of the pulse with period equal to the plasma wavelength. The degree of self-focusing seen here is probably enhanced due to the fact that our simulation geometry is planar as opposed to cylindrical. In planar geometry the power density on axis in the head of the pulse decays with time as t^{-1} instead of t^{-2} as would be expected in cylindrical geometry. This is important for the self-focusing of the body of the pulse because the head of the pulse produces the modification of the index of refraction that focuses the body of the pulse. Thus in cylindrical geometry one might see a faster erosion of the head of the pulse which eventually leads to a defocusing of the body.

Finally, Fig. 6 shows the perturbation of the index of refraction, χ, for the case of Fig. 3(c). The largest perturbations occur behind the pulse where, due to scattering, the field amplitude is very small. Thus what is plotted here is essentially the density perturbation. The relative density perturbations are quite large in this case. Indeed, it was necessary in our simulations to restrict the range of the index of refraction to prevent the density to become negative. In particular the index of refraction used in the wave equation, χ_w, was obtained from the solution of (30b) via $\chi_w=\chi/(1+\chi^2)^{1/2}$. The initial growth of the instabilities is not affected by this replacement. The restriction would not be necessary if the fully relativistic and electromagnetic equations[16] for the plasma response were calculated instead

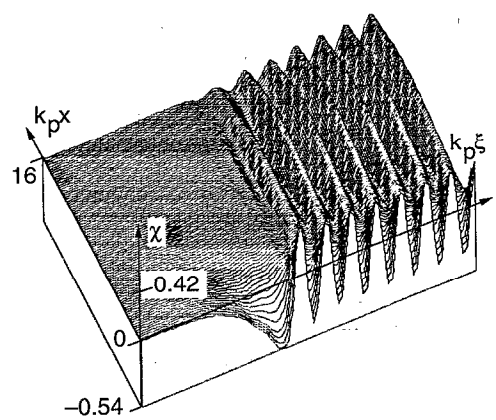

FIG. 6. Plot of the perturbation of the index of refraction, χ_w, as function of space. The parameters correspond to Fig. 3(c). Note that, for convenience, the x axis has been inverted compared to Fig. 3(c).

of the weakly relativistic equations used here. However, it should be cautioned that with such large amplitude density perturbations, multistreaming can be expected and a kinetic description of the plasma electrons is probably needed.

V. CONCLUSION

We have examined the excitation of Raman instabilities as they affect the propagation of short pulses in tenuous plasmas. Two regimes of Raman instability, corresponding to relatively large and relatively small scattering angles, are important. For the large angle case, the instability is convective in the frame of the moving pulse, and the amount of amplification increases with scattering angle. If the plasma wave-noise level is high then one can expect backscattering to be most important. Alternatively, if the seed signal for convective growth is generated by the radiation itself, then forward scattering will occur. Pulses that have passed through an aperture before they enter the plasma will contain high perpendicular wave-number components which will be transiently amplified, possibly leading to a disintegration of the pulse. The small angle scattering instability is absolute in space but convective in wave number. The instability results from a coupling of the Raman and self-focusing mechanisms, and causes the pulse to develop transverse and axial structure within a Rayleigh time. In all cases the instability becomes more severe as the length and intensity of the pulse are increased. Thus, due to these instabilities, stable pulse propagation over many Rayleigh lengths can only be expected for pulses that are not too long, $k_pL=10$–20. The trailing end of pulses which are longer than this limit will be sidescattered until the pulse is shortened to a stable length. This effect, combined with the diffraction of the head of the pulse,[7] severely limits the parameters for which effective self-focusing will occur.

A number of effects might mitigate the excitation of these instabilities, particularly the instabilities corresponding to large-angle sidescattering or backscattering. These effects include a more realistic treatment of the plasma electrons and the possible deliberate introduction of chirp in the laser pulse. The present theory has treated the excitation of plasma oscillations in the linear, cold fluid approximation. Thermal effects would tend to suppress those instabilities for which the wavelength of the plasma disturbance approached the Debye length. In practice, the temperature will probably not be high enough for this to be important,[11] but a similar effect can be expected when the pulse is intense enough to cause a macroscopic motion of the plasma. In this case, a scattered wave would encounter plasma with a spatially varying Doppler shift as it propagated out of the pulse. If the spatial variations of the Doppler shift are large enough, then the resonance between the scattered wave, the pump and the plasma wave could only be maintained over a small distance thereby reducing the amount of convective growth. A fully nonlinear treatment of the electrons is necessary to capture this effect. Likewise, the introduction of chirp in the laser pulse could spoil the resonance between the three waves. These effects can be likened to the degradation of gain in a free-electron laser with a poor quality beam, or a poor quality wiggler.

Another consideration that we have not addressed is the effect of the instability on the coherence of the wake. It may be possible that the radial and axial structure of the wake is modified by the instability and the suitability of the wake for particle acceleration needs to be studied.

Finally, due to the increase of convective amplification with scattering angle, the numerical simulation of pulse propagation becomes problematic. Indeed, the frequently employed para-axial approximation to the wave equation leads to a poorly posed problem with an ultraviolet catastrophe. This problem can be circumvented by careful control of the spatial resolution of the simulation. In doing this one introduces another parameter which is the minimum perpendicular wavelength which is allowed in the system.

ACKNOWLEDGMENTS

We acknowledge fruitful discussions with D. Pesme on various aspects of Raman instability. One of the authors (T. M. A. Jr.) would like to thank the Centre National de la Recherche Scientifique for its support and the members of the Centre de Physique Theorique of the Ecole Polytechnique for their hospitality.

APPENDIX A: RAMAN SCATTERING IN THE INFINITE HOMOGENEOUS PUMP LIMIT

In this appendix, we show the different regimes of Raman scattering in the infinite, homogeneous pump limit. Neglecting the relativistic self-focusing term in Eq. (9), we can write

$$\omega^2-\omega_p^2=\omega_p^2 a_0^2 k^2 c^2\left(\frac{1}{D_+}+\frac{1}{D_-}\right). \tag{A1}$$

In this purely temporal analysis, we assume that $\mathbf{k}$ is such that $(\omega_0-\omega_p, \mathbf{k}_0-\mathbf{k})$ exactly satisfy the dispersion relation for the light waves, i.e.,

$$\omega_p^2-k^2c^2-2(\omega_0\omega_p-\mathbf{k}\cdot\mathbf{k}_0c^2)=0.$$

We can approximate

$$D_-\approx -2(\omega_0-\omega_p)(\omega-\omega_p) \tag{A2}$$

and

$$D_+\approx 2(\omega_0+\omega_p)(\omega-\omega_p)+2(\omega_p^2-k^2c^2).$$

The quantity k can be expressed as a function of the angle of propagation θ of the scattered wave. Using an expansion in powers of ω_p/ω_0 we obtain

$$k^2c^2\approx\omega_p^2\left(1+\frac{\omega_p^2}{\omega_0^2}\right)+4\omega_0^2\sin^2\left(\frac{\theta}{2}\right),$$

and

$$D_+\approx 2(\omega_0+\omega_p)(\omega-\omega_p)-2\left(\frac{\omega_p^4}{\omega_0^2}+\omega_0^2\theta^2\right). \tag{A3}$$

It is sufficient to express the coupling term in Eq. (A1) with

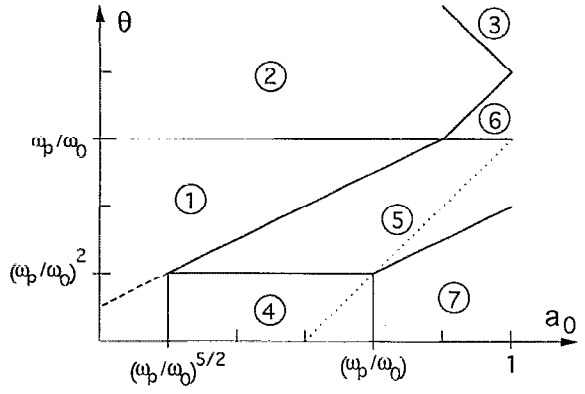

FIG. 7. Different regimes of the Raman instability in a tenuous plasma in the infinite, homogeneous pump limit.

$$k^2c^2 \approx \omega_p^2 + 4\omega_0^2 \sin^2\left(\frac{\theta}{2}\right). \tag{A4}$$

The set of equations (A1)–(A4) corresponds to seven different regimes of the instability, depending on a_0, θ, and ω_p/ω_0. For a fixed value of the ratio ω_p/ω_0, Fig. 7 shows schematically the domains corresponding to the different regimes. Domain 1 corresponds to the usual forward Raman instability with

$$\omega^2 - \omega_p^2 \approx 2\omega_p(\omega-\omega_p), \quad D_- \approx -2\omega_0(\omega-\omega_p),$$
$$|D_+| \gg |D_-|, \quad k^2c^2 \approx \omega_p^2.$$

The growth rate is

$$\gamma_1 \approx \frac{1}{2}\left(\frac{\omega_p}{\omega_0}\right)^{1/2} \omega_p a_0 .$$

Domain 2 corresponds to the Raman sidescatter, where the angular term dominates in the coupling term (A4). One has

$$\gamma_2 \approx \left(\frac{\omega_p}{\omega_0}\right)^{1/2} \omega_0 a_0 \sin\left(\frac{\theta}{2}\right).$$

Domain 3 is the Compton limit (also called strongly coupled limit[17]), where $|\omega| \gg \omega_p$, and

$$\gamma_3 \approx \frac{\sqrt{3}}{2}\left[2\omega_p^2\omega_0 \sin^2\left(\frac{\theta}{2}\right)a_0^2\right]^{1/3}.$$

So far, we have neglected the anti-Stokes contribution in (A1). This contribution has to be kept in the last four regimes. Domain 4 corresponds to the intermediate forward Raman studied by Pesme.[14] In this regime one can approximate

$$D_+ \approx 2\omega_0(\omega-\omega_p) - 2\frac{\omega_p^4}{\omega_0^2},$$

and the growth rate is

$$\gamma_4 \approx \frac{\sqrt{3}}{2}\left(\frac{1}{4}\right)^{1/3}\left(\frac{\omega_p}{\omega_0}\right)^{4/3} a_0^{2/3}\omega_p .$$

In domain 5, the angular part of the mismatch of the anti-Stokes term is dominant,

$$D_+ \approx 2\omega_0(\omega-\omega_p) - 2\omega_0^2\theta^2$$

and

$$\gamma_5 \approx \frac{\sqrt{3}}{3}\left(\frac{1}{4}\right)^{1/4}(a_0\theta)^{2/3}\omega_p .$$

Domain 6 differs from domain 5 by the fact that the angular term dominates the coupling term, so that

$$\gamma_6 \approx \frac{\sqrt{3}}{2}\left(\frac{1}{4}\right)^{1/3}\left(\frac{\omega_0}{\omega_p}a_0\theta^2\right)^{2/3}\omega_p .$$

Finally, domain 7 corresponds to the standard result for Raman forward scattering in rarefied plasma.[11,14,18] The frequency mismatch can now be neglected in the anti-Stokes contribution, and one has

$$D_- \approx -2(\omega_0-\omega_p)(\omega-\omega_p),$$
$$D_+ \approx 2(\omega_0+\omega_p)(\omega-\omega_p),$$

and

$$\gamma_7 \approx \frac{1}{\sqrt{2}}\left(\frac{\omega_p}{\omega_0}\right)\omega_p a_0 .$$

Let us now consider the modifications due to the paraxial approximations, for which

$$D_\pm = \pm 2(\omega_0\omega - \mathbf{k}_0\cdot\mathbf{k}c^2) - k_\perp^2 c^2 = 0.$$

We assume that $(\omega_0-\omega_p, \mathbf{k}_0-\mathbf{k})$ satisfy the paraxial dispersion relation, i.e.,

$$2(\omega_0\omega_p - \mathbf{k}_0\cdot\mathbf{k}c^2) - k_\perp^2 c^2 = 0.$$

Then we have

$$D_- = -2\omega_0(\omega-\omega_p)$$

and

$$D_+ = 2\omega_0(\omega-\omega_p) - 2k_\perp^2 c^2$$

with

$$k_\perp \approx \frac{\omega_0}{c}\theta,$$

and the coupling term is approximated with

$$k^2c^2 \approx \omega_p^2 + \omega_0^2\theta^2.$$

Comparing with the results obtained with the exact dispersion relation we observe that the regimes 4 and 7 disappear, and merge into regime 5. In addition, the frontier between regimes 1 and 5 is slightly modified, as shown by the dashed line on Fig. 7. Finally we note that self-focused propagation corresponds to characteristic values of $k_\perp$ of the order of $a_0\, k_p$ so that we are not interested here in the domain below the dotted line on Fig. 7. Therefore, the paraxial approximation, apart from the ultraviolet catastrophe described in the main text, is a good approximation to study the self-focusing propagation of an intense laser beam in a low-density plasma.

APPENDIX B: OUTGOING WAVES

We wish to solve Eq. (30a) subject to the condition at the boundary $x=X_{\max}$ that waves leave the system without reflection. We assume that for $x>X_{\max}$ the perturbation of the index of refraction is negligible and we set the right-hand side of Eq. (30a) to zero. The outgoing wave-boundary condition is easily enforced on the temporal Laplace transform of the field amplitude $a(x,\xi,s)$,

$$\left.\frac{\partial a}{\partial x}\right|_{x=X_{\max}} = i\left(\frac{2is\omega_0}{c^2}\right)^{1/2} a(x=X_{\max},s).$$

The problem is then to find a way to enforce this condition in the time domain. In principle, this requires carrying out a convolution over time of all past values of the field amplitude at the boundary in order to determine the correct value of the derivative of the field amplitude. This is then repeated at each time step. Because a convolution of this type is not numerically efficient, we use an alternate procedure. In particular, we represent the square root of the Laplace transform variable as a sum of rational poles,

$$\sqrt{\frac{s}{w}} \approx \sum_{n=1}^{10} \frac{\sigma_n}{(s/w)+\gamma_n} - \sum_{n=1}^{10} \frac{\sigma_n}{\gamma_n},$$

where the poles, γ_n, were chosen to satisfy a geometric progression with values between 0.05 and 4.0, and the values of the ten coefficients σ_n, were chosen to minimize the integral of the square error defined by the difference of the two terms appearing on either side of the equality in the above,

$$\int_{-w}^{+w} d\omega \left| \sqrt{\frac{i\omega}{w}} - \left(\sum_{n=1}^{10} \frac{\sigma_n}{(i\omega/w)+\gamma_n} - \sum_{n=1}^{10} \frac{\sigma_n}{\gamma_n} \right) \right|^2.$$

Here, w is a scale factor which gives the range of frequencies over which the boundary is nonreflecting.

With the above replacement, the boundary condition in the time domain is expressed as

$$\left.\frac{\partial a}{\partial x}\right|_{x=X_{\max}} = i\left(\frac{2iw\omega_0}{c^2}\right)^{1/2} \times \left(\sum_{n=1}^{10} g_n - a(x=X_{\max},s) \sum_{n=1}^{10} \frac{\sigma_n}{\gamma_n} \right),$$

where the variables g_n satisfy ordinary differential equations in time

$$\frac{dg_n}{dt} + \gamma_n g_n = \sigma_n a(\xi, X_{\max}, t).$$

With this approximate boundary condition, we were able to successfully enforce outgoing waves over the range of frequencies encountered in the simulations.

[1] P. Maine, D. Strickland, P. Bado, M. Pessot, and G. Mourou, IEEE J. Quantum Electron. **QE-24**, 398 (1988).
[2] T. Tajima and J. M. Dawson, Phys. Lett. **43**, 267 (1979); L. M. Gorbunov and V. I. Kirsanov, Zh. Eksp. Teor. Fiz. **93**, 509 (1987) [Sov. Phys. JETP **66**, 290 (1987)].
[3] M. S. Sodha, A. K. Ghatak, and V. K. Tripathi, in *Progress in Optics*, edited by E. Wolf (North-Holland, Amsterdam, 1976), Vol. 13, p. 169; E. M. Epperlein, Phys. Rev. Lett. **65**, 2145 (1990).
[4] P. Kaw, G. Schmidt, and T. Wilcox, Phys. Fluids **16**, 1522 (1973); C. E. Max, *ibid.* **19**, 74 (1976); B. I. Cohen, B. F. Lasinski, A. B. Langdon, and J. C. Cummings, Phys. Fluids B **3**, 766 (1991).
[5] G. Schmidt and W. Horton, Comments Plasma Phys. Controlled Fusion **9**, 85 (1985).
[6] G. Z. Sun, E. Ott, Y. C. Lee, and P. Guzdar, Phys. Fluids **30**, 526 (1987); W. B. Mori, C. Joshi, J. M. Dawson, D. W. Forslund, and J. M. Kindel, Phys. Rev. Lett. **60**, 1298 (1988); T. Kurki-Suonio, P. J. Morrison, and T. Tajima, Phys. Rev. A **40**, 3230 (1989); P. Gibbon, Phys. Fluids B **2**, 2196 (1990); A. B. Borisov, A. V. Borovskiy, V. V. Korobkin, A. M. Prokhorov, O. B. Shiryaev, X. M. Shi, T. S. Luk, A. McPherson, J. C. Solem, K. Boyer, and C. K. Rhodes, Phys. Rev. Lett. **68**, 2309 (1992); P. Sprangle, C. M. Tang, and E. Esarey, IEEE Trans. Plasma Sci. **PS-15**, 145 (1987).
[7] P. Sprangle, E. Esarey, and A. Ting, Phys. Rev. Lett. **64**, 2011 (1990).
[8] C. E. Max, J. Arons, and A. B. Langdon, Phys. Rev. Lett. **33**, 209 (1974).
[9] A. Ting, P. Sprangle, and E. Esarey, in *Advanced Accelerator Concepts*, edited by C. Joshi, AIP Conf. Proc. No. 193 (American Institute of Physics, New York, 1989), p. 398.
[10] J. F. Drake, P. K. Kaw, Y. C. Lee, G. Schmidt, C. S. Liu, and M. N. Rosenbluth, Phys. Fluids **17**, 778 (1974); W. M. Manheimer and E. Ott, *ibid.* **17**, 1413 (1974); R. Pellat, in *Laser–Plasma Interaction*, Proceedings of the Les Houches Summer School, Session XXXIV, edited by R. Balian and J. C. Adam (North-Holland, Amsterdam, 1982), p. 411.
[11] C. J. McKinstrie and R. Bingham, Phys. Fluids B **4**, 2626 (1992).
[12] P. Sprangle and E. Esarey, Phys. Rev. Lett. **67**, 2021 (1991).
[13] T. M. Antonsen, Jr. and P. Mora, Phys. Rev. Lett. **69**, 2204 (1992).
[14] See National Technical Information Service Document No. PB92100304 (Interaction Laser Matière 1986 Report by D. Pesme, pp. 21–32). Copies may be ordered from the National Technical Information Service, Springfield, Virginia 22161.
[15] A. Bers, in *Handbook of Plasma Physics*, edited by M. N. Rosenbluth and R. Z. Sagdeev, *Volume I–Basic Plasma Physics*, edited by A. A. Galeev and R. N. Sudan (North-Holland, New York, 1983) p. 451.
[16] P. Breizman, D. L. Fisher, P. Z. Chebotaev, and T. Tajima (private communication, 1991).
[17] C. B. Darrow, C. Coverdale, M. D. Perry, W. B. Mori, C. Clayton, K. Marsh, and C. Joshi, Phys. Rev. Lett. **69**, 442 (1992).
[18] K. Estabrook and W. L. Kruer, Phys. Fluids **26**, 1892 (1983).